Bearing capacity of plane-strain footings on layered soils

H.J. Burd and S. Frydman

Abstract: A study has been carried out of the bearing capacity of sand layers overlying clay soils for the case where the thickness of the sand layer is comparable to the width of a rigid foundation placed on the soil surface. A review of previous work is given and a discussion is presented of the dimensionless groups that govern the behaviour of this type of foundation. A parametric study is carried out using both finite element and finite difference methods. This study is based on the use of soil parameters obtained from an assessment of the range of values that might be expected to be appropriate for full-scale structures. The results of the parametric study are used to illustrate the mechanics of the system and also to develop charts that may be used directly in design. In particular, the results illustrate that the shear strength of the clay has an important influence on the mechanisms of load spread within the fill.

Key words: bearing capacity, layered soils, numerical analysis.

Résumé : L'on a réalisé une étude sur la capacité portante de couches de sable reposant sur des sols argileux pour le cas où l'épaisseur de la couche de sable est comparable à la largeur d'une fondation rigide posée sur la surface du sol. L'on présente une revue des travaux antérieurs et une discussion sur les groupes sans dimension qui régissent le comportement de ce type de fondation. Une étude paramétrique est réalisée en utilisant les méthodes tant des éléments finis que des différences finies. Cette étude est fondée sur l'utilisation des paramètres de sols obtenus en partant de l'évaluation de la plage des valeurs que l'on pourrait s'attendre à trouver dans des structures à pleine échelle. Les résultats de l'étude paramétrique ont été utilisés pour illustrer le mécanisme du système et aussi pour développer des abaques qui peuvent être utilisées directement dans la conception. En particulier, les résultats illustrent que la résistance au cisaillement de l'argile a une influence importante sur les mécanismes de répartition de la charge à l'intérieur du remblai.

Mots clés : capacité portante, sols multicouches, analyse numérique.
[Traduit par la rédaction]

Introduction

The bearing capacity of a vertically loaded footing placed on the surface of a homogeneous soil may be estimated relatively easily using conventional Terzaghi bearing capacity theory in which appropriate values of the bearing capacity factors are adopted. This type of calculation is based on the implicit assumption that the soil is rigid-perfectly plastic with the strength characterized by a cohesion and an angle of friction. Whilst this approach is highly successful for homogeneous soils, it cannot, in general, be used for cases where the soil properties vary with depth.

Naturally occurring soils are often deposited in layers. Within each layer the soil may, typically, be assumed to be homogeneous, although the strength properties of adjacent layers are generally quite different. If a foundation is placed on the surface of a layered soil for which the thickness of the top layer is large compared with the width of the foundation, then realistic estimates of the bearing capacity may be obtained using conventional bearing capacity theory based on the properties of the upper layer. If the thickness of the top layer is comparable to the foundation width, however, this approach may not be appropriate.

Several important examples exist of foundation engineering problems in which it may be necessary to include the effect of soil layers in an assessment of bearing capacity. Shallow offshore foundations, for example, generally have large physical dimensions; potential failure surfaces may therefore extend a significant distance below the soil surface. Any soil layers within the depth of these failure surfaces would be expected to influence the failure load. (A discussion of the behaviour of jack-up foundations placed on layered soils is given by Craig and Chua 1990.) Other examples include structures placed on engineered fill layers (e.g., oil storage tanks, which may be founded on a thin layer of granular fill) and unpaved roads built on soft clays where a layer of compacted fill is used to spread the load applied by passing vehicles.

This paper deals with the specific case of the bearing capacity of a rigid plane-strain footing placed on the surface of a soil consisting of a uniform sand layer overlying a thick, homogeneous bed of clay, as shown in Fig. 1. The study is restricted to cases where the thickness of the sand layer, D, is comparable to the footing width, B, and in all cases the ground surface and the interface between the two soil layers is horizontal. The assumption is made that the response of the clay layer is undrained and the response of the sand layer is drained. A discussion is given of the various analytical models that have been proposed for this type of analysis. A detailed description is then given of a numerical parametric study that has been

Received April 3, 1996. Accepted December 9, 1996.

H.J. Burd. Department of Engineering Science, Parks Road, Oxford OX1 3PJ, U.K.
S. Frydman. Faculty of Civil Engineering, Technion, Israel Institute of Technology, Haifa, Israel.

Fig. 1. Footing on layered soil.

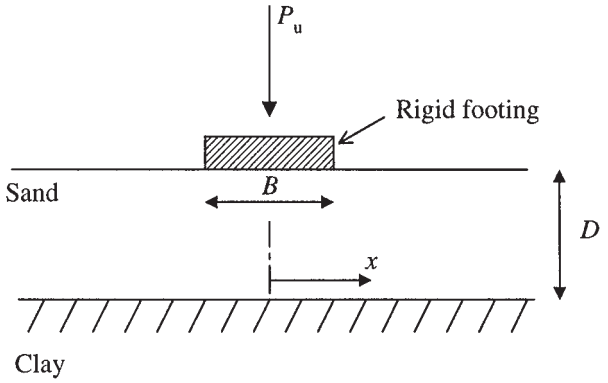

Fig. 2. Load spread mechanism.

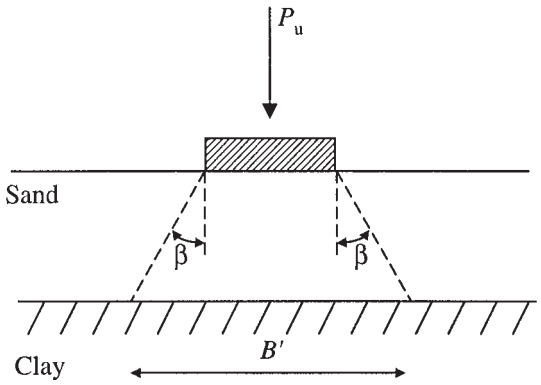

carried out to investigate the mechanics of this problem. To specify the parametric study, the various parameters and dimensionless groups that influence the bearing capacity are identified. By making certain assumptions, and by introducing various standard correlations, the number of independent variables is shown to reduce to five dimensionless groups.

Analytical design models

Load spread models

One widely used approach to estimate the bearing capacity of sand layers overlying clay is to assume that the sand acts to spread the load beneath the footing and that the foundation fails when bearing capacity failure occurs within the clay. This procedure is clearly only appropriate for cases where the strength of the sand layer is substantially greater than that of the clay.

The load spread mechanism within the sand layer may be modelled relatively simply by assuming that the vertical stresses associated with the footing load are confined to a zone defined by lines inclined at angle β to the vertical, as shown in Fig. 2. Load from the footing is assumed to be distributed uniformly over a width B' at the base of the sand layer, where $B' = B + 2D \tan \beta$. Although the chosen value of β can have an important influence on the calculated bearing capacity, it is often not clear how its value should be selected. In practice, a value of β of $\tan^{-1}$ 0.5 is often adopted (Houlsby et al. 1989), although it is generally accepted that the value of this parameter will be influenced by the strength of the sand. Brocklehurst (1993) further showed that the value of β is strongly influenced by the strength of the clay.

Fig. 3. Punching shear model (Meyerholf 1974).

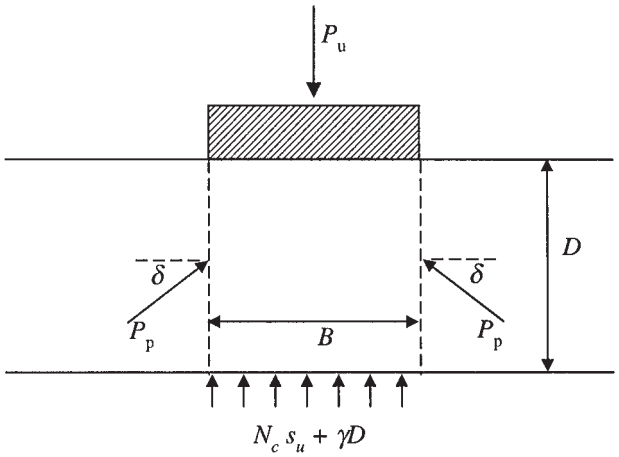

The bearing capacity, P_u, may be estimated using the expression:

$$[1] \quad P_u = B' s_u N_c$$

where s_u is the undrained shear strength of the clay, and N_c is the standard bearing capacity factor for undrained loading. Houlsby et al. (1989), however, suggested that the shear stresses that develop at the base of the sand layer tend to reduce the vertical bearing capacity of the clay. They also proposed a procedure by which these shear stresses may be calculated and used to estimate a modified bearing capacity factor for use in [1].

An alternative model for load spread through the sand was proposed by Bourdeau (1989) based on an analysis for load spread through a particulate layer initially given by Harr (1977). This analysis suggested that normal stresses at the base of the sand layer may be obtained by appropriate superposition of Gaussian distribution functions. This approach was used by Bourdeau (1989) to study the behaviour of a reinforced granular layer placed on an elastic soil, but does not appear to have been extended to the case of a granular layer overlying clay.

Punching shear models

Meyerhof (1974) proposed an alternative model of behaviour for this type of problem. In this model, the bearing capacity of a strip footing placed on the soil surface is estimated by considering a simplified mechanism in which the sand is assumed to be in a state of passive failure along a vertical plane beneath each edge of the footing, as shown in Fig. 3. Immediately beneath the footing, the vertical stress acting on the clay is assumed to be $N_c s_u + \gamma D$, where N_c is a suitable bearing capacity factor and γ is the unit weight of the sand. A passive force, P_p, inclined at an angle δ is assumed to act on the vertical planes beneath the footing edges, giving an expression for the footing bearing capacity:

$$[2] \quad P_u = B N_c s_u + 2 P_p \sin \delta$$

Meyerhof (1974) suggested that the value of P_p may be obtained from the expression:

$$[3] \quad P_p = \frac{\frac{1}{2}\gamma D^2 K_p}{\cos \delta}$$

where the value of K_p, the passive earth pressure coefficient, at the appropriate value of sand friction angle, ϕ', may be obtained from standard solutions (e.g., Kerisel and Absi 1990). Meyerhof suggested that the value of δ would be expected to vary within the depth of the sand layer and proposed the use of an average value of $2\phi'/3$.

Hanna and Meyerhof (1980) showed that when the clay layer is relatively weak, passive failure of the sand layer may be accompanied by a failure surface that extends downwards into the clay. In this case, values of K_p obtained by assuming that failure is confined to the sand layer will be too large. Hanna and Meyerhof used a limit-equilibrium approach to study this case and obtained values for a coefficient of punching shear, K_s, which is related to K_p by the equation $K_p \tan \delta = K_s \tan \phi'$. They presented the results of the analysis in the form of charts in which the relationship between K_s and ϕ' is plotted as a function of the clay shear strength, s_u, and the ratio δ/ϕ'. These charts are not presented in a nondimensional form, however, and so are appropriate only for the values of sand unit weight and layer thickness that were adopted in their preparation (Burd and Frydman 1996). Furthermore, the precise details of the limit-equilibrium calculation used by Hanna and Meyerhof are not clear, and so it is not straightforward to repeat their analysis.

The punching shear model proposed by Meyerhof (1974) and Hanna and Meyerhof (1980) is based on well-established theory and provides a useful insight into the behaviour of granular soils overlying clay. This model may be compared to a simple load spread approach if it is assumed that the load from the footing is spread over a total width B' at the base of the sand and that the bearing stress at the clay surface is $N_c s_u + \gamma D$. The punching shear model then gives:

$$[4] \quad B' = B + \frac{\gamma D^2 K_s \tan \phi'}{N_c s_u}$$

This corresponds to the value of load spread angle given by:

$$[5] \quad \tan \beta = \left(\frac{\gamma D}{s_u}\right)\left(\frac{K_s \tan \phi'}{2N_c}\right)$$

Equation [5] suggests that the value of β depends on the sand friction angle, as might be expected. Perhaps surprisingly, however, the equation also suggests that the value of load spread angle may be a function of the dimensionless group $s_u/\gamma D$. It is shown later in this paper that this particular dimensionless group has an important influence on the bearing capacity of this type of layered soil foundation.

A common feature of the punching shear model and the simple load spread model described above is the assumption that the bearing capacity of the clay is unaffected by the vertical stresses applied to the clay surface immediately outside of the loaded area. Madhav and Sharma (1991) discussed this point and showed that the bearing capacity immediately beneath the footing may be significantly enhanced when the vertical stresses acting on the clay surface decay gradually with distance from the footing rather than reducing abruptly. Madhav and Sharma (1991) considered various surcharge cases and deduced that, for bearing capacity problems of this type, the general nature of the load distribution at the interface between the sand and the clay may increase the bearing capacity of the clay immediately beneath the footing by up to 30%.

Kinematic analyses

Several authors have described the use of kinematic analysis methods to obtain approximate solutions to this type of problem. Florkiewicz (1989), for example, presented solutions for a range of cases involving both cohesive and cohesionless soils. Michalowski and Shi (1995) used a similar approach to carry out an extensive parametric study of the specific case of sand overlying clay; the results were presented in the form of design charts. Burd and Frydman (1996) studied the Michalowski and Shi (1995) solutions over a limited range of variables and concluded that they may significantly overestimate the bearing capacity. This tendency to overestimate is not surprising (as pointed by Michalowski and Shi (1996)) and is partly due to the assumption inherent in the Michalowski and Shi (1995) design charts that the sand is a fully associated material. Kinematic analyses may be demonstrated to provide upper bound solutions only for the case of associated materials, whereas the dilation angle of real granular soils is generally substantially less than the angle of friction. An analysis that adopts a dilation angle equal to the friction angle will also provide an upper bound to the correct solution for a nonassociated material, but this upper bound will probably become increasingly conservative as the difference between the two angles increases. For the case of a nonassociated material, an admissible kinematic solution may be obtained by using a modified friction angle (Davis 1968; Drescher and Detournay 1993), but this solution cannot be proven to be an upper bound.

Numerical models

In principle, several of the major difficulties associated with the use of the analysis approaches described above are solved automatically by the use of numerical procedures such as finite element or finite difference methods in which the soil is subdivided into a mesh of discrete elements. These procedures employ algorithms that ensure that both equilibrium and compatibility requirements are satisfied, or at least closely approximated, within the soil mass during the course of the calculation. The methods suffer from the important disadvantage, however, that the nature of the discretization adopted in the analysis may lead to errors in the solution. If the calculations are carried out with care, however, these errors can often be reduced to acceptably small levels.

Many of the previous attempts to develop numerical models of the behaviour of footings on layered soils (e.g., Love et al. 1987; Griffiths 1982*a*; Brocklehurst 1993) were based on the use of a finite element method. It is well known that bearing capacity calculations pose severe difficulties for finite element analysis, particularly for the case of shallow foundations on sand (e.g., Frydman and Burd 1997). One of the sources of these difficulties is the additional kinematic constraints imposed on the system by the specified volumetric strains associated with plastic flow (Sloan 1981; Sloan and Randolph 1982). The detrimental effect of these constraints may be reduced by choosing appropriate element types or, alternatively, by using reduced or selective integration procedures. In addition, analyses involving

the bearing capacity of frictional materials are often prone to instability (e.g., Griffiths 1982*b*) particularly when the friction angle is large. It is possible, with care, however, to obtain reliable solutions using numerical modelling, and this is attempted in the study described in the present paper.

Parametric study using finite element and finite difference methods

To assess the various analytical procedures reviewed above, and to provide data of direct use in design, a parametric study has been carried out using two distinct numerical modelling procedures. The use of two independent numerical procedures allows a realistic judgement to be made about the consistency and reliability of the results.

The parametric study was carried out using finite element and finite difference analyses. The finite element calculations were carried out using the program OXFEM, which has been developed at Oxford University, U.K., and the finite difference calculations were performed using the commercial program FLAC (ITASCA Consulting Group, Inc. 1993). All of the finite element calculations were based on six-noded triangular elements with a three-point Gauss integration rule to calculate the element stiffness matrices. The solution algorithm was based on a tangent stiffness approach employing a modified Euler procedure. Full details of these algorithms are discussed by Burd (1986). FLAC (Fast Lagrangian Analysis of Continua) uses an explicit, time marching method to solve the governing field equations, in which every derivative is replaced by an algebraic expression written in terms of field variables (e.g., stress or displacement) at discrete points in space; these variables are undefined elsewhere.

Specification of the parametric study

In this study, the sand layer was treated as a linear elastic-perfectly plastic (frictional) material and the clay was assumed to be linear elastic-perfectly plastic (cohesive). This approach clearly would not be appropriate to model cases where progressive failure or strain softening is important. It is thought, however, that this simplified model of behaviour may give useful and realistic results that are appropriate for a range of applications of shallow foundations on layered soils.

It is known that the bearing capacity of footings on sand is strongly influenced by the nature of the interface between the base of the footing and the soil. In all of the calculations described in this paper the footing was assumed to be perfectly rough. The study of smooth footings is beyond the scope of this paper, although it might be expected that the performance of smooth and rough footings would be different. The results of the parametric study indicate, however, that the mobilized friction angle on the base of the footing is generally significantly smaller than the friction angle of the granular layer, and so the assumption that the interface is fully rough is thought to be a realistic one for most foundation applications. The rough footing condition was enforced in the numerical analyses by prescribing a downward displacement of the footing while preventing horizontal movement of the nodes in contact with the base of the footing.

The behaviour of the sand is defined by a shear modulus, G_s, Poisson s ratio, ν_s, plane-strain friction angle, ϕ', and plane-strain dilation angle, ψ. The parameters needed to specify the model adopted for the clay are shear modulus, G_c, Poisson s ratio, ν_c, and plane-strain undrained shear strength, s_u. In addition it is necessary to specify the unit weights of the soils and the values of coefficient of lateral earth pressure at the start of each analysis.

A total of 13 parameters are needed to define each analysis, as listed below:

Problem geometry: B, D
Sand properties: G_s, ν_s, ϕ', ψ, γ
Clay properties: G_c, ν_c, s_u, γ_c
Initial stress ratios: $(K_o)_s$, $(K_o)_c$

where γ and γ_c are the unit weights of the sand and the clay, respectively, and $(K_o)_s$ and $(K_o)_c$ are the coefficients of lateral earth pressure for the sand and the clay. Note that this list includes various parameters that are known not to influence the bearing capacity of homogeneous soils (i.e., values of soil stiffness, Poisson s ratio, clay unit weight, and coefficient of lateral earth pressure). It would be expected that the value of the unit weight of the clay would not be an important parameter for the layered soil problem. It is not immediately clear, however, whether the effect of several of the other parameters (for example the stiffness of the sand and $(K_o)_s$) may also be assumed to be negligible.

The behaviour of the sand layer would be expected to be influenced strongly by its friction angle and, to a lesser extent, by its angle of dilation. The dilation angle of sand, ψ, is known to be related to the peak friction angle, ϕ'_p, and the critical state friction angle, ϕ'_c; an expression of the form given below is widely accepted (e.g., Bolton 1986) and is adopted for these calculations:

$$[6] \qquad 0.8\psi = \phi'_p - \phi'_c$$

If it is assumed that, at failure, the mobilized friction angle within the failure zone corresponds to the peak value, then it would be appropriate to set the friction angle of the sand, ϕ', to be equal to the peak friction angle, ϕ'_p. For a quartz sand, a value of ϕ'_c of 32° is thought to be appropriate, and this value was adopted for the calculations in association with [6]. The parametric study was based on the use of three different values of ϕ': 32°, 40°, and 48°. In each case, [6] was used to obtain suitable values of the dilation angle for use in each analysis.

The value of ν_s is not thought to vary substantially for sand layers of different types, or to have a significant influence on the bearing capacity. A constant value of 0.2 was therefore adopted for all the calculations. The clay was assumed to be incompressible (corresponding to undrained behaviour of a fully saturated material). The use of a clay Poisson s ratio of 0.5, however, would lead to numerical difficulties, and so, as is conventional, a slightly lower value (of 0.49) was adopted. The value of $(K_o)_c$ is not thought to be important, and a value of unity was adopted in all of the analyses. Values of the coefficient of lateral earth pressure for the sand were obtained from the Jaky expression:

$$[7] \qquad (K_o)_s = 1 - \sin\phi'$$

It is generally accepted that [7] is appropriate only for cases where the sand is normally consolidated. However, a numerical investigation in which $(K_o)_s$ was varied suggested that this parameter does not have any significant influence on the computed bearing capacity.

If the relationships described above are adopted and the variables collected into dimensionless groups, then the mean

footing pressure, p, at bearing capacity failure may be shown to be given by the functional form:

$$[8] \quad \frac{p}{\gamma B} = f\left(\frac{B}{D}, \frac{s_u}{\gamma D}, \frac{G_s}{G_c}, \phi'\right)$$

The dimensionless group $s_u/\gamma D$ is referred to in this paper as the "shear strength ratio." Its importance has been noted previously in the context of bearing capacity of layered soils (Craig and Chua 1990), and it was shown earlier in this paper to be relevant when interpreting a simple punching shear approach in terms of a load spread model. This group will be recognized as the stability number used in the analysis of cuttings, and it is linked closely to the overconsolidation ratio of the clay. This latter aspect must be borne in mind, as discussed later, in the choice of appropriate combinations of parameters for use in the analyses.

It is well accepted that the plane-strain, undrained shear strength of a clay may be reasonably represented by an expression of the form (Ladd et al. 1977):

$$[9] \quad \left(\frac{s_u}{\sigma'_v}\right) = \left(\frac{s_u}{\sigma'_v}\right)_{nc} \mathrm{OCR}^{\Lambda}$$

where σ'_v is the effective overburden stress, OCR is the overconsolidation ratio expressed in terms of vertical effective stresses, and $(s_u/\sigma'_v)_{nc}$ is the normally consolidated undrained shear strength ratio. Typical values for Λ and the normally consolidated undrained shear strength ratio are 0.8 and 0.3, respectively. If these values are adopted, then the plane-strain undrained shear strength is given by:

$$[10] \quad s_u = 0.3\sigma'_v \, \mathrm{OCR}^{0.8}$$

Before a footing load is applied to the sand surface, the effective overburden stress at the top surface of the clay is γD. The corresponding value of clay shear strength is:

$$[11] \quad \frac{s_u}{\gamma D} = 0.3 \, \mathrm{OCR}^{0.8}$$

Realistic values of the shear strength ratio may, therefore, be obtained by adopting suitable values of OCR. Values of OCR adopted in the parametric study and corresponding values of undrained shear strength ratio calculated from [11] are given in Table 1.

The calculations described in this paper were all based on a clay soil in which the strength remains constant with depth; this feature of the analysis is consistent with the conventional Terzaghi bearing capacity factor approach. It is possible that variations in clay strength with depth may have an important influence on the bearing capacity of the foundation; the extension of these calculations to cases where the strength of the clay is nonhomogeneous, however, is beyond the scope of this paper.

Equation [8] suggests that the bearing capacity of the layered system may be a function of the ratio G_s/G_c. To obtain realistic values of this ratio for use in the parametric study, a procedure was adopted in which values of G_c and G_s were estimated independently and their ratio taken. This procedure is described below.

Typical values of G_c/s_u for each value of OCR adopted in the parametric study were selected from data given by Wroth et al. (1979) and are listed in Table 1. Unfortunately, the shear

Table 1. Values of clay shear properties.

OCR	$s_u/\gamma D$	G_c/s_u
1	0.3	160
4.5	1	79
25	4	28
60	8	25
100	12	23

modulus of sand is less well documented than that of clay, although it is known to depend strongly on the magnitude of both the stresses and the strains, with the stiffness increasing with increasing stress level and reducing as the shear strain increases. The small strain shear modulus is commonly related to mean effective stress, p', by an expression of the form (Wroth et al. 1979):

$$[12] \quad \frac{G_s}{p_a} = K\left(\frac{p'}{p_a}\right)^n$$

where p_a is atmospheric pressure, K is a constant depending on the void ratio, and n is a constant, usually assumed to lie in the range $1/3 < n < 1$. For the case of a layer of sand, it is convenient to express [12] in terms of the current vertical effective stress, σ'_v, rather than the mean effective stress, in which case the following relationship is suggested:

$$[13] \quad \frac{G_s}{p_a} = K^*\left(\frac{\sigma'_v}{p_a}\right)^n$$

where the constants K^* and K are closely related. For normal values of voids ratios, K^* would be expected to be about 700. For the present analyses, in which the sand beneath the footing reaches failure and so it may be assumed that shear strains are relatively large, the nonlinear dependence of G_s on shear strain must be considered. Wroth et al. (1979) suggested that at a shear strain magnitude of 1.0%, the value of G_s can be expected to about 5% of its small strain value. The appropriate value of K^* would therefore be about 35. For the purposes of this study, the value of K^* was assumed to lie in the range 20 to 45.

It is assumed, for simplicity, that when a surface footing is applied to the sand and the clay is in a state of bearing capacity failure, the vertical stresses in the sand are of the order of $(\pi + 2)s_u$. If, for convenience, the value of n for use in [13] is taken as unity, then suitable values of G_s may be found for each value of s_u used in the study. On this basis, the value of G_s/G_c was found to be about 1 for $s_u/\gamma D = 0.3$ and about 8 for $s_u/\gamma D = 12$, appropriate values of G_s and G_c for use in the analyses were chosen accordingly. In fact, a few preliminary analyses indicated that changes in the stiffness ratio did not have a significant effect on the analysis results. In view of this, no attempt was made to study in further detail the effect of variations of the shear modulus ratio on the system performance.

The main parametric study considered values of B/D ranging from 1.5 to 0.75; these values were chosen to focus the study on foundations in which the fill thickness is comparable with the footing width. The values of shear strength ratio adopted in this main study were 0.3, 1, and 4, which correspond to values of OCR of about 1, 4.5, and 25. It is thought that these values span the range of clay overconsolidation ratios that might

Fig. 4. Finite element for $B/D = 1$: (*a*) mesh, (*b*) detail near footing.

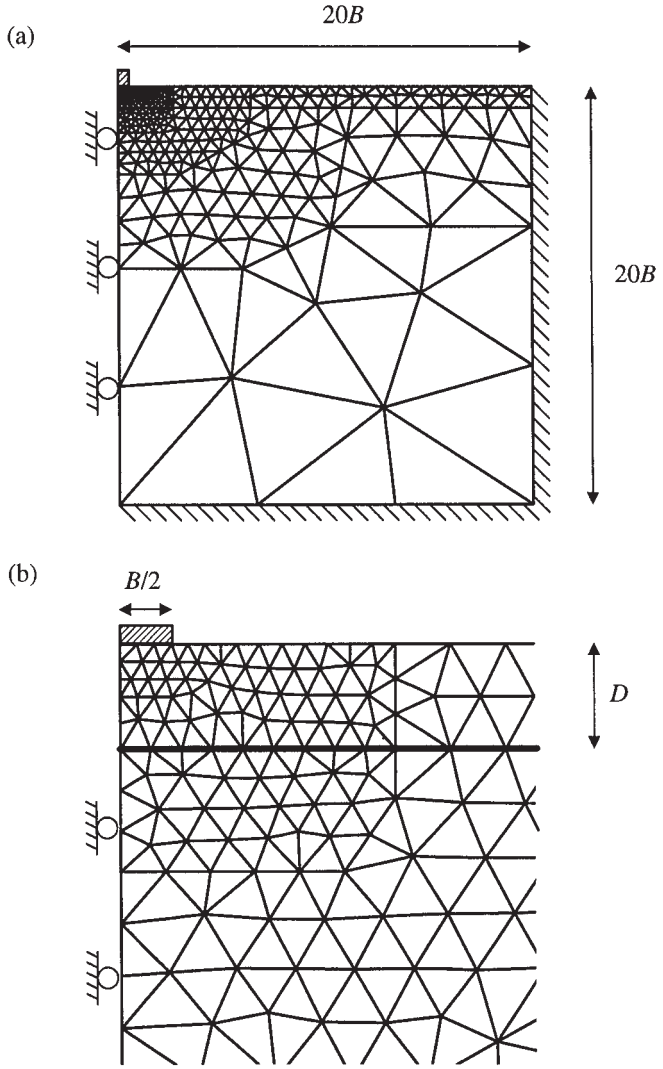

Fig. 5. FLAC mesh for $B/D = 1$: (*a*) mesh, (*b*) detail near footing.

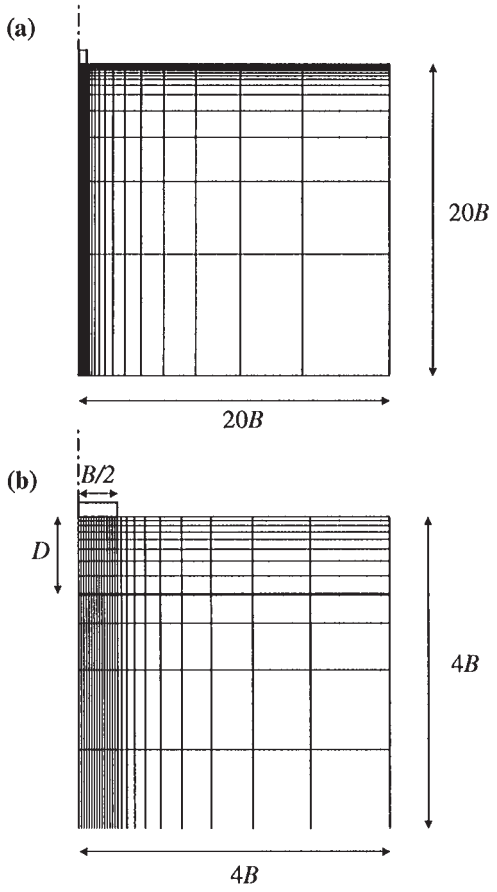

be expected in practice. Three values of friction angle, ϕ' were adopted: 32°, 40°, and 48°. These values were thought to be appropriate to model loose, medium-dense, and dense quartz sand, respectively. For the case where $\phi' = 40°$, several additional FLAC runs were carried out in order to investigate the behaviour of the system for sand layers of increased thickness and for values of shear strength ratio up to 12. Although shear strength ratios in excess of about 4 correspond to values of OCR that are unusually high, these calculations were performed in order to extend the results obtained from the main study.

Numerical procedures

All of the analyses were based on meshes of overall dimension 20*B* by 20*B*, where *B* is the footing width. Typical meshes adopted in the OXFEM and FLAC analyses are shown in Figs. 4 and 5, respectively. In each calculation, a set of prescribed, vertical displacements was applied in increments to the nodes at the base of the footing, and the resulting footing pressure was obtained by summing the vertical nodal loads at the base of the footing and then dividing by the footing half-width. The bearing capacity was obtained in each case from the limiting value of footing pressure that developed as the footing displacement increased.

Fig. 6. Comparison between FLAC and OXFEM results.

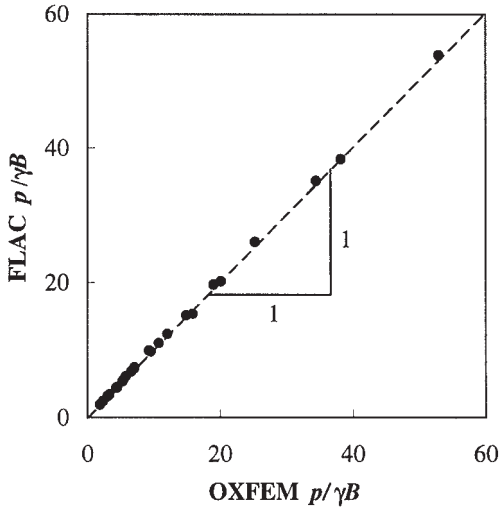

Considerable care was taken to ensure that numerical errors associated with the analyses were acceptably small. The meshes were designed such that the elements were concentrated in highly stressed zones and the boundaries were sufficiently distant from the footing to ensure that the mesh

Fig. 7. Variation of $p/\gamma B$ with $s_u/\gamma D$. (Main parametric study.)

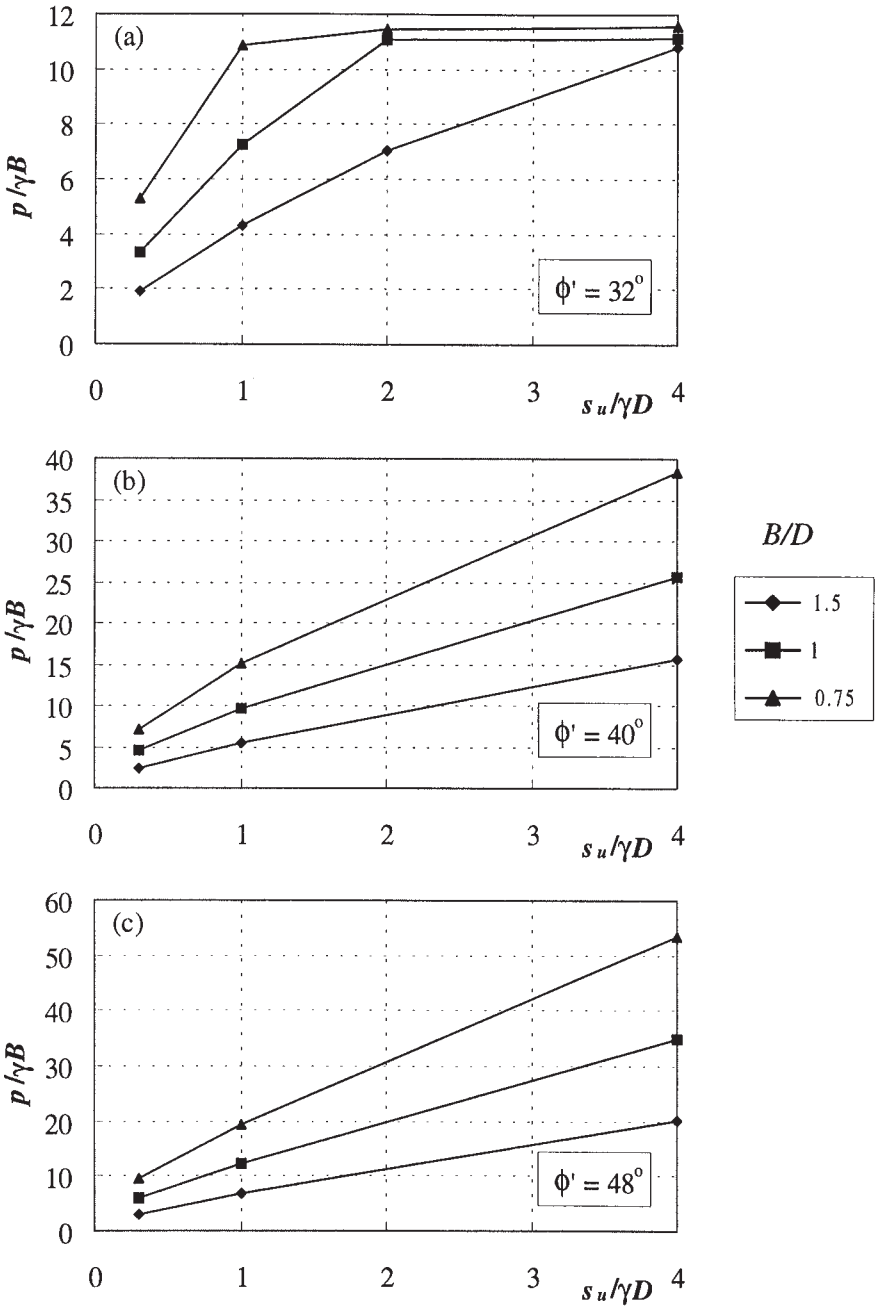

contained the entire plastic zone. The number of calculation increments was chosen to ensure that equilibrium errors remained small, and several of the calculations were repeated with different meshes to ensure that discretization errors were not excessive. These measures were consistent with recommendations made on the basis of a previous study of the bearing capacity of homogeneous sand (Frydman and Burd 1997).

Results

Most of the main parametric study calculations were carried out using both FLAC and OXFEM. Figure 6 shows a comparison between the values of bearing capacity, p, obtained using the two procedures and illustrates the excellent agreement that was obtained. This consistency provides some confidence in the reliability of the results obtained from the study.

Plots of nondimensionalised bearing capacity

The results of the main parametric study are presented in Fig. 7 in terms of $p/\gamma B$ (the bearing capacity ratio) plotted against $s_u/\gamma D$ (the shear strength ratio). These plots are based on the use of the average values of bearing capacity obtained from the OXFEM and FLAC analyses, except for the few cases where only FLAC data were obtained.

It is clear from Fig. 7 that for $\phi' = 32°$ the bearing capacity ratio initially increases with increasing shear strength ratio (for constant B/D) and that for $B/D = 1.0$ and 1.5 the bearing capacity

Fig. 8. Variation of $p/\gamma B$ with $s_u/\gamma D$ for $\phi' = 40°$.

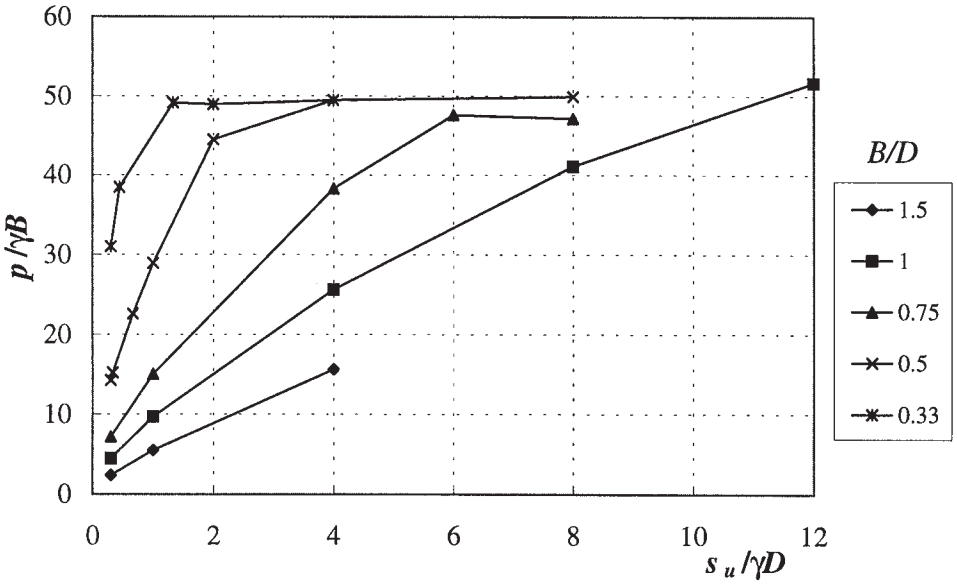

reaches an upper limit that appears to be independent of $s_u/\gamma D$. This suggests that at low values of shear strength ratio the failure mechanism extends into the clay, and that as the shear strength ratio is increased beyond a certain value, the failure surface becomes confined to the sand layer. The results shown in Fig. 7 suggest that for $\phi' = 40°$ and $\phi' = 48°$ the failure surface extends into the clay layer in all cases. Figure 8 shows the results of additional calculations for $\phi' = 40°$, in which relatively large values of shear strength ratio and also two additional sand thicknesses ($B/D = 0.33$ and $B/D = 0.5$) were considered. These data show a similar pattern to the $\phi' = 32°$ case, in which the bearing capacity ratio tends to reach a plateau value as the shear strength ratio is increased. The general pattern of these results is broadly in line with the kinematic analysis solutions presented by Michalowski and Shi (1995) and Florkiewicz (1989).

The effect of increasing the clay strength on the shape and size of the failure surface for the case where $\phi' = 40°$ and $B/D = 0.5$ is shown in Figs. 9*a* to 9*c*, which show the envelope of the plastic zone, obtained from the FLAC analyses, for values of shear strength ratio of 4, 2, and 0.67. It is seen that for $s_u/\gamma D = 4$, the failure zone is confined entirely to the sand layer, and for the lower values of shear strength ratio, the failure zone extends into the clay.

Meyerhof (1974) suggested that for a two-layer system, for the particular case when the failure mechanism is known to be confined to the upper layer, the bearing capacity may be estimated from the expression:

[14] $$p = 0.5\gamma B N'_\gamma$$

where N'_γ is a bearing capacity factor that depends, in general, on the thickness, D, of the upper layer as well as the sand friction angle. If D is greater than the depth, h, of the failure mechanism for a homogeneous soil with properties equal to those of the sand, then N'_γ is set equal to the conventional bearing capacity factor N_γ based on the friction angle of the upper layer. If D is less than h, however, then Meyerhof suggested that appropriate values of N'_γ for the case of a rough footing may be obtained from solutions given by Mandel and Salençon (1972). It should be noted that the condition $D \geq h$ does not necessarily imply that failure is confined to the upper layer because even in this case the failure mechanism may extend into the lower layer if the clay is sufficiently weak. In this case Meyerhof s approach would, clearly, not be applicable.

Figure 7 shows that for $\phi' = 32°$ the bearing capacity reaches an upper limit for $B/D = 0.75$ and 1.0 and Fig. 8 indicates similar behaviour for $\phi' = 40°$ and $B/D = 0.33$, 0.5, and 0.75. The depth of failure, h, in a deep, homogeneous, sand layer may be estimated from data given by Mandel and Salençon (1972) to be given by $B/h = 1.19$ for $\phi' = 32°$ and 0.81 for $\phi' = 40°$ (the first of these two values was obtained from Mandel and Salençon s data by interpolation). This suggests that, provided $B/D < 1.19$ for $\phi' = 32°$ and $B/D < 0.81$ for $\phi' = 40°$, the bearing capacity of the system for cases where failure is confined to the upper layer may be obtained using [14] in conjunction with N_γ. This condition is satisfied by all of the cases in Figs. 7 and 8 where the bearing capacity reaches a limiting value. For $\phi' = 32°$ and 40°, Frydman and Burd (1997) showed that appropriate values of N_γ for a rough strip footing are about 26 and 96, respectively. On this basis, upper limits of bearing capacity ratio of 13 and 48 would be expected. The upper limits indicated in Figs. 7 and 8 for $\phi' = 32°$ and 40° are seen to be reasonably consistent with these values.

Results obtained during this parametric study indicated that, for cases where failure is confined to the sand layer, the computed bearing capacity is generally highly sensitive to changes in mesh topology. Figure 8, for example, shows that the limiting bearing capacity ratios obtained for $B/D = 0.33$ and 0.5 are close, but about 5% higher than the values obtained for $B/D = 0.75$. This variability is associated with differences in the FLAC meshes used for the analyses. The meshes used for $B/D = 0.5$ and $B/D = 0.75$ both contained nine rows of elements within the sand layer, with the element size increasing with distance from the top of the mesh, as shown in Fig. 5 (for $B/D = 1$). The portion of the mesh within the sand layer for $B/D = 0.75$ was therefore finer than for $B/D = 0.5$, leading to

lower and presumably more accurate values of limiting bearing capacity. The $B/D = 0.33$ mesh, however, contained 11 rows of elements within the sand and was designed so that the arrangement of elements within the sand layer matched closely that adopted for $B/D = 0.5$. As would be expected, the computed limiting bearing capacities were similar. For cases where the failure extends into the clay layer, the analysis was found to be better conditioned and the solutions were less sensitive to the precise form of the mesh.

The limiting values of bearing capacity ratio obtained by Michalowski and Shi (1995) were approximately 11, 24, 60, and 160 for friction angles of 30°, 35°, 40°, and 45°, respectively. These limits correspond to the case where $D \geq h$, and so the values would be expected to be equal to $0.5N_\gamma$. Data given by Frydman and Burd (1997) suggest that appropriate values for N_γ are 16.6, 40, 96, and 264. Michalowski and Shi s values for the limiting bearing capacity ratio would, therefore, appear to be unconservative, by a factor of between 20% and 30%.

The load spread angle

The data from the parametric study are plotted in an alternative way in Fig. 10 in order to illustrate the mechanisms of load spread within the fill. In these plots the parameter β is obtained from the expression:

$$[15] \quad \tan\beta = \frac{\frac{pB}{s_u N_c} - B}{2D}$$

where N_c is set equal to $\pi + 2$ (i.e., the conventional value of bearing capacity for undrained loading). The values of β calculated in this way are consistent with the load spread model illustrated in Fig. 2. This load spread model is based on a highly simplified view of the mechanics of the system, and so particular values of β may not have a precise physical interpretation. However, interpretation of the numerical results in terms of the load spread angle, β, allows a useful impression to be gained of the effectiveness of the sand layer in transmitting the footing load to the clay. The load spread model becomes inappropriate when failure is confined to the sand layer, and so Fig. 10 contains only those results for which the bearing capacity ratio is less than the limiting values shown in Figs. 7 and 8. Figure 10 shows, as expected, that the value of β tends to increase with increasing angle of friction. The results also show that β is remarkably insensitive to the value of the fill thickness. There is, however, a clear dependence on the shear strength ratio, with the load spread angle tending to reduce significantly as the value of $s_u/\gamma D$ increases. Figure 10*b*, for example, shows that for a fill with a friction angle of 40°, the appropriate value of β varies from about 45° for a normally consolidated clay to zero, with increasing clay strength.

The results indicated by Fig. 10 may have important practical consequences. For cases where the physical dimensions of the problem are relatively small, as might be the case for a conventional shallow foundation, the clay is likely to be overconsolidated, and so $s_u/\gamma D$ will be relatively large. In these cases the fill layer is likely to be considerably less effective in spreading the applied load than might be expected in, for example, a large offshore foundation where the clay would be expected to be normally consolidated or lightly overconsolidated. It is clear, therefore, that it is necessary to ensure correct scaling of the shear strength ratio in order to apply the results of small-scale laboratory studies of the behaviour of foundations on layered soils to the behaviour of full-scale structures.

Fig. 9. Lower envelope of plastic zone, B/D = 0.5, $\phi' = 40°$, for (*a*) $s_u/\gamma D = 4$; (*b*) $s_u/\gamma D = 2$; and (*c*) $s_u/\gamma D = 0.67$.

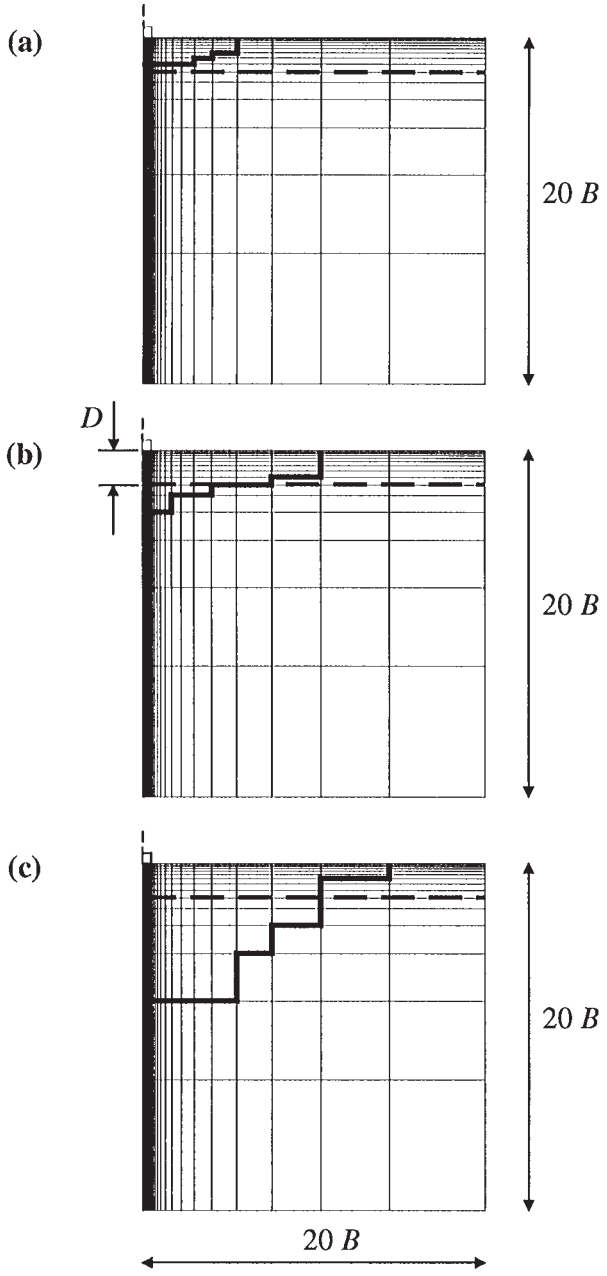

Figure 11 illustrates the pattern of normal stresses applied to the clay surface in terms of the nondimensional parameter $\eta = (q_c - \gamma D)/(N_c s_u)$, where q_c is the normal stress acting on the surface of the clay and $N_c = (\pi + 2)$. This figure shows values of η for the case where $B/D = 1.0$, $\phi' = 40°$, and $s_u/\gamma D$ varies from 0.3 to 12. Figure 12 gives a plot of the shear stress, τ_c, acting on the clay surface for the same set of analyses. These data were all obtained from analyses carried out using FLAC. In all cases the data were extracted by sampling the stress points in the elements immediately below the sand–clay interface. Figure 11 shows that, for $s_u/\gamma D = 12$, the value of η on the footing centre

Fig. 10. Variation of β with $s_u/\gamma D$.

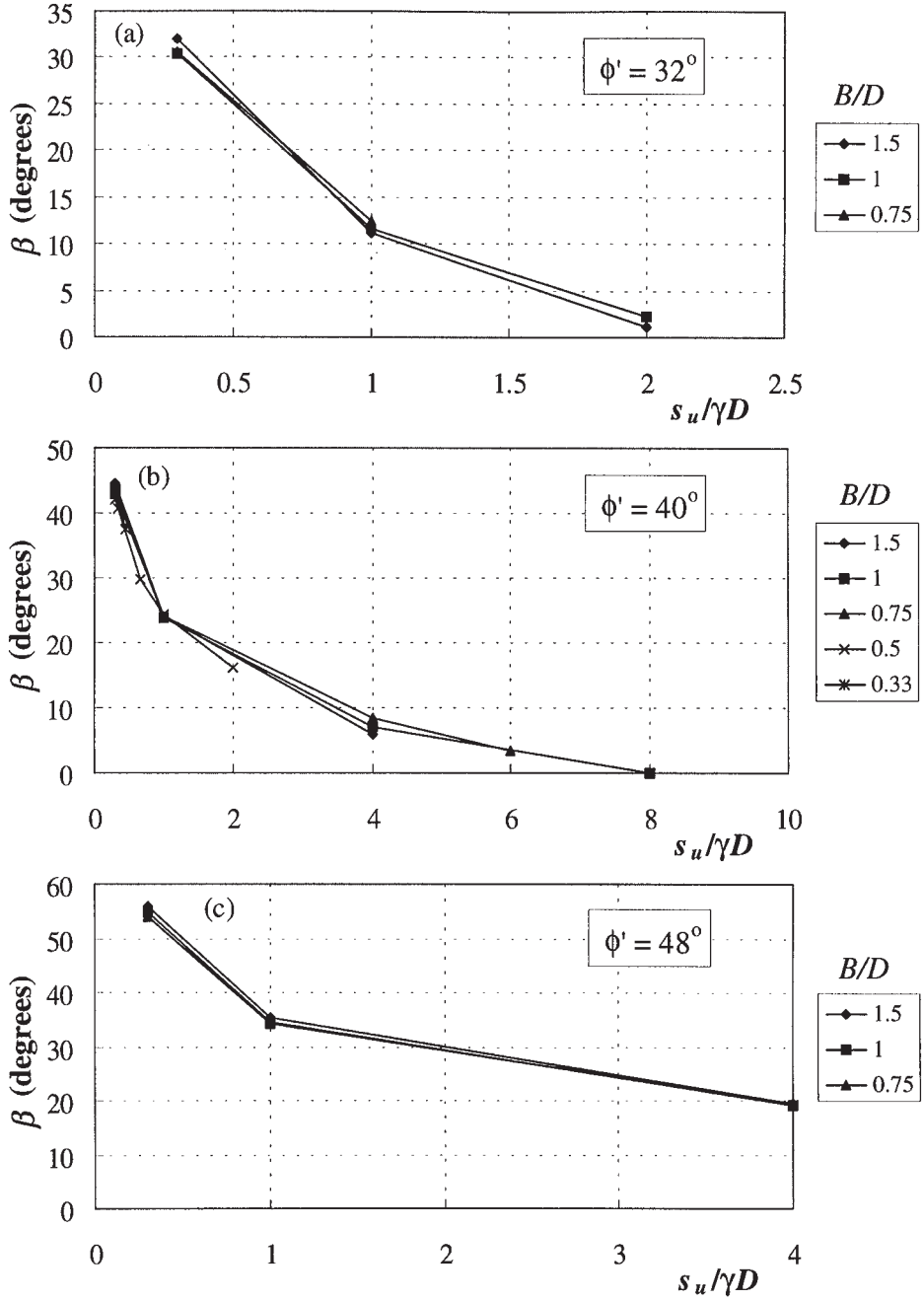

line (i.e., at $x = 0$) is significantly less than the value of unity that might be expected from a conventional bearing capacity analysis of the clay. This is consistent with the results plotted in Fig. 8, which suggest that, for this case, the failure mechanism is confined to the sand layer. For values of $s_u/\gamma D = 4$, 1, and 0.3, the failure surface is thought to extend into the clay, and in these cases the value of η on the footing centre line is equal to, or greater than, unity. This feature of behaviour would be expected (Madhav and Sharma 1991) as a consequence of the general distribution of the normal stresses applied to the clay. In all cases, Figs. 11 and 12 indicate that the normal stresses tend to decay with distance from the footing centre line, and that the greatest rate of decay occurs in the region below the footing edge where the shear stresses reach a maximum. This suggests that the outward acting shear stresses developed beneath the footing tend to reduce the local bearing capacity of the clay, a feature of the system that is discussed in detail by Houlsby et al. (1989). Figure 11 also shows that as the shear strength ratio is reduced, the width over which appreciable vertical stresses are applied to the clay surface tends to increase. This indicates that the sand layer becomes more effective in spreading the load applied by the footing as the shear strength ratio is reduced and is consistent with the general pattern shown in Fig. 10.

It is clear from Fig. 12 that, for values of shear strength ratio in excess of about 1, the distribution of shear stresses acting

Fig. 11. Normal stresses acting on clay surface.

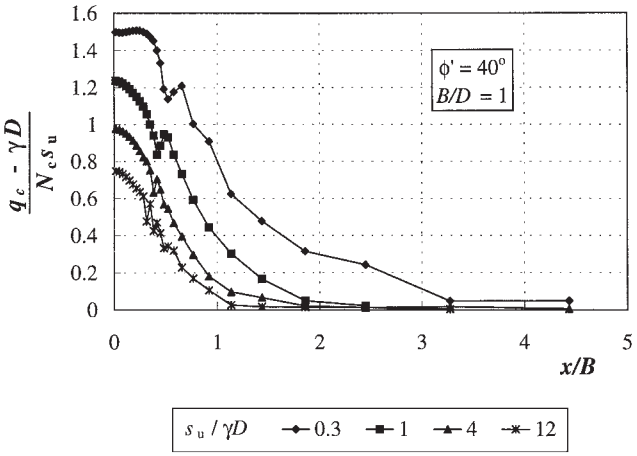

Fig. 12. Shear stresses acting on clay surface.

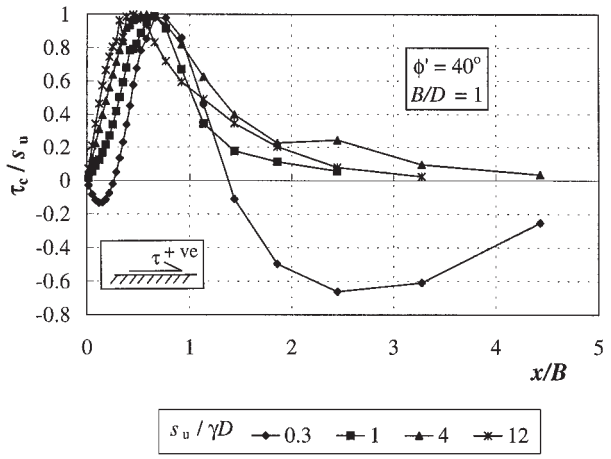

Fig. 13. Variation of normal stress beneath the footing.

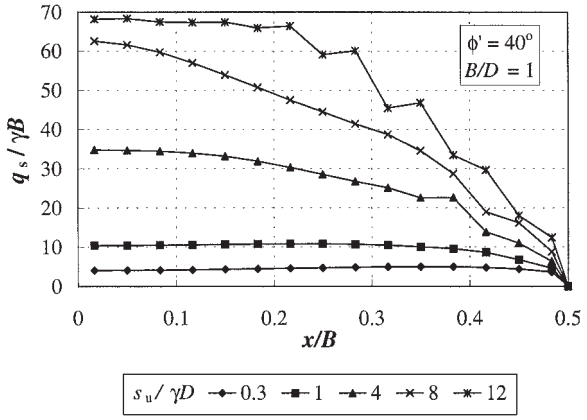

Fig. 14. Variation of shear stress beneath the footing.

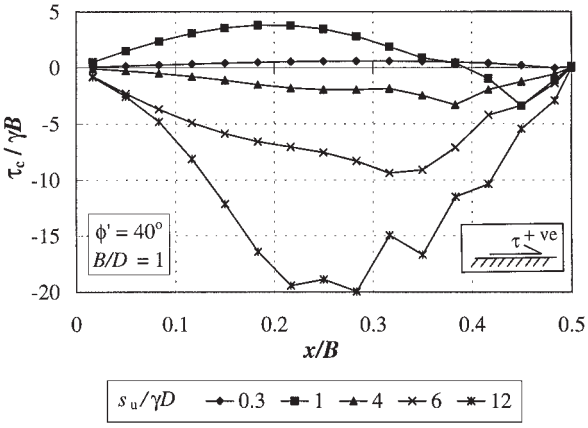

on the clay surface does not depend significantly on the shear strength ratio. The pattern is different for a shear strength ratio of 0.3; in this case it is seen that for $x > 1.5B$, a substantial amount of negative (i.e., inward acting) shear is applied to the clay. This is associated with the tendency of the clay to squeeze outwards. When the clay is very soft, the strength of the sand is sufficient to apply restraint to this lateral movement.

Figures 13 and 14 show the normal stress, q_s, and horizontal shear stress, τ_s, applied to the sand immediately beneath the footing for $\phi' = 40°$ and $B/D = 1$. For a shear strength ratio of 12, when the failure zone is confined to the sand layer, the stress distributions are similar to those observed for a footing on a homogeneous sand layer (Frydman and Burd 1997). In this case, the normal stress is maximum at the footing centre line, remains reasonably constant over about half of the footing width, and then decreases, gradually, to zero at the edge. The shear stresses applied to the sand in this case act towards the centre of the footing. As the clay shear strength decreases, and failure therefore begins to extend into the clay, a reduction in the general magnitude of the normal stresses occurs. The distribution also changes with the normal stress, tending to become nearly uniform. The pattern of shear stresses shows a marked change as the shear strength ratio is reduced substantially. For the two lower strengths considered ($s_u/\gamma D = 1$ and 0.3) the shear stresses change sign and act on the top of the sand in an outward direction. The tendency of the sand beneath the footing to move inwards in this case is presumably associated with failure and plastic flow of the clay beneath the footing.

Conclusions

A detailed parametric study has been carried out on the bearing capacity of a sand layer overlying clay. The study is based on a careful assessment of appropriate combinations of soil properties and has been performed using two independent numerical methods.

The study has highlighted the fundamental importance of the nondimensional group $s_u/\gamma D$ in determining the mechanics of the system. This group is closely related to the overconsolidation ratio of the clay and allows a realistic range of clay shear strength values to be adopted in the study.

The results of the study have been used to produce charts of bearing capacity that may be used directly in design. The data have also been used to discuss the mechanics of the system and, in particular, to study the effectiveness of the sand in spreading the load applied by the footing. This load spread mechanism may be characterized by a load spread angle β. It is shown that β increases with increasing sand friction angle,

as might be expected, and that it also tends to reduce significantly as the shear strength ratio is increased. This latter feature suggests that the sand layer is considerably more effective in spreading the footing load when the clay is normally or lightly overconsolidated, than when the overconsolidation ratio of the clay is large. For the values of B/D adopted in the study, the value of β is shown to be insensitive to the sand thickness.

Several previously proposed analytical procedures for this type of problem have been discussed. Load spread models are shown to be a useful framework for understanding the mechanics of the problem, although in any practical application, they suffer from the important disadvantage that it is difficult to estimate the load spread parameter in advance. The punching shear models proposed by Meyerhof (1974) and Hanna and Meyerhof (1980) are also considered. In principle, methods of this sort provide a useful analytical tool, although the design charts for the punching shear coefficient given by Hanna and Meyerhof (1980) are not presented in nondimensionalized form, and this limits their application. Useful design charts that cover a broad range of parameters are given by Michalowski and Shi (1995). These solutions, by their very nature, are upper bounds, and they may overestimate the bearing capacity by a significant amount.

References

Bolton, M.D. 1986. The strength and dilatancy of sands. Géotechnique, **36**(1): 65–78.

Bourdeau, P.L. 1989. Modelling of membrane action in a two-layer reinforced soil system. Computers and Geotechnics, **7**: 19–36.

Brocklehurst, C.J. 1993. Finite element studies of reinforced and unreinforced two-layer soil systems. D.Phil. thesis, University of Oxford, Oxford, U.K.

Burd, H.J. 1986. A large displacement finite element analysis of a reinforced unpaved road. D.Phil. thesis, University of Oxford, Oxford, U.K.

Burd, H.J., and Frydman, S. 1996. Discussion on bearing capacity of footings over two-layer foundation soils. Journal of Geotechnical Engineering, ASCE, **122**(8): 699–700.

Craig, W.H., and Chua, K. 1990. Deep penetration of spud-can foundations on sand on clay. Géotechnique, **40**(4): 541–556.

Davis, E.H. 1968. Theories of plasticity and the failure of soil masses. *In* Soil mechanics: selected topics. *Edited by* I.K. Lee. Butterworth, London, U.K., pp. 341–380.

Drescher, A., and Detournay, E. 1993. Limit load in translational failure mechanisms for associative and non-associative materials. Géotechnique, **43**(3): 443–456.

Florkiewicz, A. 1989. Upper bound to bearing capacity of layered soils. Canadian Geotechnical Journal, **26**: 730–736.

Frydman, S., and Burd, H.J. 1997. Numerical studies of the bearing capacity factor N_γ. Journal of Geotechnical Engineering, ASCE, **123**(1): 20–29.

Griffiths, D.V. 1982*a*. Computation of bearing capacity on layered soils. Proceedings, 4th International Conference on Numerical Methods in Geomechanics, Vol. 1, pp. 163–170.

Griffiths, D.V. 1982*b*. Computation of bearing capacity factors using finite elements. Géotechnique, **32**(3): 195–202.

Hanna, A.M., and Meyerhof, G.G. 1980. Design charts for ultimate bearing capacity of foundations on sand overlying soft clay. Canadian Geotechnical Journal, **17**: 300–303.

Harr, M.E. 1977. Mechanics of particulate media. McGraw-Hill, New York.

Houlsby, G.T., Milligan, G.W.E., Jewell, R.A., and Burd, H.J. 1989. A new approach to the design of unpaved roads—Part 1. Ground Engineering, **22**(3): 25–29.

ITASCA Consulting Group, Inc. 1993. FLAC—Fast Lagrangian Analysis of Continua. Minneapolis, Minn.

Kerisel, J., and Absi, E. 1990. Active and passive earth pressure tables. 3rd. ed. A.A. Balkema, Rotterdam.

Ladd, C.C., Foott, R., Ishihara, K., Poulos, H.G., and Schlosser, F. 1977. Stress-deformation and strength characteristics. State Of The Art Report for Session 1, 11th International Conference on Soil Mechanics and Foundation Engineering, Tokyo.

Love, J.P., Burd, H.J., Milligan, G.W.E., and Houlsby, G.T. 1987. Analytical and model studies of reinforcement of a layer of granular fill on a soft clay subgrade. Canadian Geotechnical Journal, **24**: 611–622.

Madhav, M.R., and Sharma, J.S.N. 1991. Bearing capacity of clay overlain by stiff soil. Journal of Geotechnical Engineering, ASCE, **117**(12): 1941–1948.

Mandel, J., and Salençon, J. 1972. Force portante d un sol sur une assise rigide (étude théorique). Géotechnique, **22**(1); 79–93.

Meyerhof, G.G. 1974. Ultimate bearing capacity of footings on sand layer overlying clay. Canadian Geotechnical Journal, **11**: 223–229.

Michalowski, R.L., and Shi, L. 1995. Bearing capacity of footings over two-layer foundation soils. Journal of Geotechnical Engineering, ASCE, **121**(5): 421–428.

Michalowski, R.L., and Shi, L. 1996. Bearing capacity of footings over two-layer foundation soils: closure. Journal of Geotechnical Engineering, ASCE, **122**(8): 701–702.

Sloan, S.W. 1981. Numerical analysis of incompressible and plastic solids using finite elements. Ph.D. thesis, University of Cambridge, Cambridge, U.K.

Sloan, S.W., and Randolph, M.F. 1982. Numerical prediction of collapse loads using finite element methods. International Journal for Numerical and Analytical Methods in Geomechanics, **6**: 47–76.

Wroth, C.P., Randolph, M.F., Houlsby, G.T., and Fahey, M. 1979. A review of the engineering properties of soils with particular reference to the shear modulus. Cambridge University Engineering Department Report CUED/D - Soils TR75.

List of symbols

B	footing width
B'	width of loaded area on clay surface
D	thickness of sand layer
G_c	shear modulus of clay
G_s	shear modulus of sand
h	depth of the failure mechanism
$(K_o)_c$	coefficient of lateral earth pressure for clay
$(K_o)_s$	coefficient of lateral earth pressure for sand
K_p	coefficient of passive earth pressure
K_s	coefficient of punching shear
N_c	bearing capacity factor
N_γ	bearing capacity factor
p	mean footing pressure at failure
p_a	atmospheric pressure
p'	mean effective stress
$p/\gamma B$	bearing capacity ratio
q_c	normal stress applied to clay surface
q_s	normal stress applied to sand surface
P_u	footing load at failure
P_p	passive force
s_u	undrained shear strength of clay
$s_u/\gamma D$	shear strength ratio
x	horizontal distance from footing centre line

σ'_v effective overburden stress
τ_c shear stress applied to clay surface
τ_s shear stress applied sand surface
β load spread angle
η nondimensional vertical stress applied to clay
γ unit weight of sand
γ_c unit weight of clay
ν_c Poisson s ratio of clay
ν_s Poisson s ratio of sand
ψ dilation angle of sand
ϕ' effective friction angle of sand
ϕ'_p peak friction angle
ϕ'_c critical state friction angle